CONF-880917--2

UCRL- 98768
PREPRINT

UCRL--98768

DE90 008357

MAGNETIC RECONNECTION SIMULATION USING THE 2.5D EM DIRECT IMPLICIT CODE AVANTI

Dennis W. Hewett
Gregory E. Francis
Claire E. Max

This paper was prepared for submittal to the
International Workshop on Reconnection in
Space Plasma to be held in Potsdam, East Germany
September 5-9, 1988.

August 30, 1988

Lawrence Livermore National Laboratory

MAGNETIC RECONNECTION SIMULATION USING THE 2.5D EM DIRECT IMPLICIT CODE AVANTI

Dennis W. Hewett, Gregory E. Francis, and Claire E. Max
Physics Department and
Institute of Geophysics and Planetary Physics
Lawrence Livermore National Laboratory
University of California

ABSTRACT

Collisionless reconnection of magnetic field lines depends upon electron inertia effects and details of the electron and ion distribution functions, thus requiring a kinetic description of both. Though traditional explicit PIC techniques provide this description in principle, they are severly limited in parameters by time step constraints. This parameter regime has been expanded by using the recently constructed 2.5 D electromagnetic code AVANTI in this work. The code runs stably with arbitrarily large Δt and is quite robust with respect to large fluctuations occurring due to small numbers of particles per cell. We have found several qualitatively new features. The reconnection process is found to occur in distinct stages: 1) early spontaneous reconnection fed by the free energy of an initial anisotropy in the electron component, 2) coalescence of the resulting small-scale filaments of electron current, accompanied by electron jetting, and 3) oscillatory flow of electrons through the magnetic X-point, superposed on continuing nonlinear growth of ion-mediated reconnection. The time evolution of stage 3) is strongly dependent on M_i/m_e.

Keywords: Collisionless Reconnection, Implicit PIC Simulation

1. INTRODUCTION

We report here continued research[1] on the evolution of magnetic field reconnection in a collisionless plasma neutral sheet, using *implicit particle-in-cell computer simulations*. The general two-dimensional collisionless neutral sheet configuration is thought to be of relevance to the magnetotails of the earth and other magnetized planets, where reconnection is associated with magnetic sub-storms;[2] and to the eventual fate of tangled magnetic field lines in collisionless astrophysical plasmas, in which estimates of the thermal conductivity depend sensitively on the largely unknown rate of field-line reconnection.[3] The specific parameters of our simulation are quite close to plasma conditions in the laboratory reconnection experiments of Stenzel and Gekelman.[4]

In simplest form reconnection in a *collisional* plasma can be modeled using the MHD equations with a fixed value for the plasma resistivity. This yields a reduced, one-fluid description in which the large-scale topology and dynamics of reconnecting regions can be studied. By contrast, *collisionless* reconnection of magnetic field lines depends on electron inertia effects and the detailed behavior of the electron distribution function to provide the neces-

sary freedom for magnetic topology changes. The formation of a non-Maxwellian tail on the ion distribution can be an important observed consequence of collisionless reconnection. Hence a faithful computational model must include a kinetic description of both electrons and ions.

Altnough traditional explicit particle-in-cell (PIC) techniques provide this description, stability requirements restrict simulation parameters to artificially small ion-to-electron mass ratios (e.g. $M_i/m_e \approx 10$ to 25), and short temporal periods (e.g. 100 plasma periods ω_{pe}^{-1} or less)[5]. In the present paper a new 2.5D fully electromagnetic Direct Implicit PIC plasma simulation code AVANTI[6] allows us to follow the dynamics of collisionless reconnection for all relevant M_i/m_e, and for a factor of 2 to 3 longer timescales. The code runs stably with arbitrarily large Δt and is quite robust with respect to large fluctuations occurring due to small numbers of particles per cell. This code is ideally suited for studies of magnetic reconnection because of the increased flexibility in time step selection. High frequency electron plasma oscillations that are immaterial to magnetic reconnection need not be resolved numerically. Similarly, purely electromagnetic modes are unimportant in this process and are not resolved. We select the appropriate time step, typically $\omega_{pe}\Delta t \approx$ 1-2, needed to give detailed resolution of electron gyro-motion and other particle-field interactions that are important to collisionless reconnection. Further details of this method can be found in Hewett and Langdon[6] and references therein. Overall, we estimate that this implicit technique has expanded the parameter regime that can be studied by at least an order of magnitude.

The simulation region consists of a 40x96 x-y mesh, with all quantities initially uniform in y. Starting with a constant ion temperature and a Gaussian ion density profile we derive the initial equilibrium fields shown in Figure 1(a). The initial neutral sheet width δ is $2c/\omega_{pe}$. Larmor radii for electrons and ions outside of the neutral sheet are $\rho_e = 0.4c/\omega_{pe}$ and $\rho_i = 20c/\omega_{pe}$, respectively. By way of comparison, the laboratory reconnection experiments of Stenzel and Gekelman[7] typically use $\delta = 3c/\omega_{pe}$, $\rho_e = 0.4c/\omega_{pe}$ and $\rho_i = 2c/\omega_{pe}$. The x-gradient in magnetic pressure near the neutral sheet is balanced by gradients in electron and ion particle density. Periodic boundary conditions are imposed at the top and bottom of the box. At the sides of the box, fields and particle densities approach values that are constant with x. Boundary conditions at the sides are perfect reflection for particles, Dirichlet conditions for E, and Neumann conditions for B.

This equilibrium resembles the Harris equilibrium,[8] but the ions carry no current, and are electrostatically confined. We also allow for anisotropy in electron temperatures parallel ($T_{e\parallel}$) and perpendicular ($T_{e\perp}$) to the initial magnetic field. Following the work of Chen and Palmadesso,[9] we allow a cooler $T_{e\parallel}$ to trigger the initial stages of reconnection.

2. SIMULATION RESULTS

Figure 1(b-d) shows the time evolution of the magnetic field topology for a typical simulation. Contours of magnetic flux are shown as solid lines; the innermost (dotted) contour is the "separatrix", inside of which lies magnetic

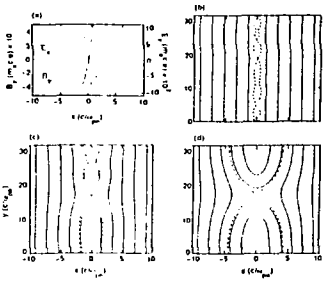

Figure 1. a) Profiles of initial electrostatic field E_z (dashed) and magnetic field B_y (solid) across the neutral sheet. Both fields have units of $m_e c\omega_{pe}c/e$. The sheet current in the x direction is carried by electrons. Ions are contained by the electrostatic field. The initially uniform electron and ion temperatures are $T_{e\perp}/m_e c^2 = 2.8 \times 10^{-2}$, $T_{e\parallel} = (1/9)T_{e\perp}$, $T_i/m_e c^2 = 8.0 \times 10^{-2}$. (b-d): Magnetic flux contours (solid) and separatrix (dotted) in x-y plane: (b) At $t = 30\omega_{pe}^{-1}$, showing small-scale electron-driven filaments; (c) At $t = 160\omega_{pe}^{-1}$, as coalescence begins; (d) At $t = 410\omega_{pe}^{-1}$, with only one X-point remaining.

flux that has become trapped due to reconnection. Frame 1(b) shows the magnetic configuration characteristic of the early stages of reconnection, before the ions have had time to move. The electron current at the neutral sheet has already formed small-scale filaments, resulting in several magnetic X-points within the simulation volume. Later, Figure 1(c) shows that some of these small-scale filaments have coalesced. Still later, when enough time has passed for ion dynamics to become important, we see one remaining magnetic island, as in Figure 1(d). This stage of the process is typically reached in aproximately 1-3 Alfvén transit times. The remaining O-point continues to grow in amplitude, for our parameters, until the separatrix approaches the boundaries of the simulation box. The simulation is then terminated; further results would be artifacts of the boundary conditions.

A normal component of the electric field (E_z) develops as the small-scale current filaments coalesce; this field is consistent with the $\mathbf{E} \times \mathbf{B}$ drift of the electrons (but not the unmagnetized ions) into the final O-point through the X-point. The resulting electron current in the x-y simulation plane generates a normal component of the magnetic field (B_z) with quadrupole structure. Shown in Fig. 2 are the a) contours of E_z and b) B_z at the same time as Fig. 1d contours. Hoshino[10] showed that the suppression of this quadrupole field does not affect the rate of magnetic reconnection, suggesting that B_z is not a cause, but an effect, of the reconnection process.

Simulations with large ion-electron mass ratio ($M_i/m_e \geq 200$) reveal an oscillation in the sign of the normal B_z quadrupole. The cause is an oscillation in the electron flow through the X-point. Since the magnetic field is "frozen" into the electron component, the magnitude of trapped magnetic flux will also oscillate as the electrons flow into and out of the O-point. Observation of trapped flux as a function of time for various M_i/m_e provides information about the moderating influence of the ions on the electron oscillation. This temporial behavior is consistent with the

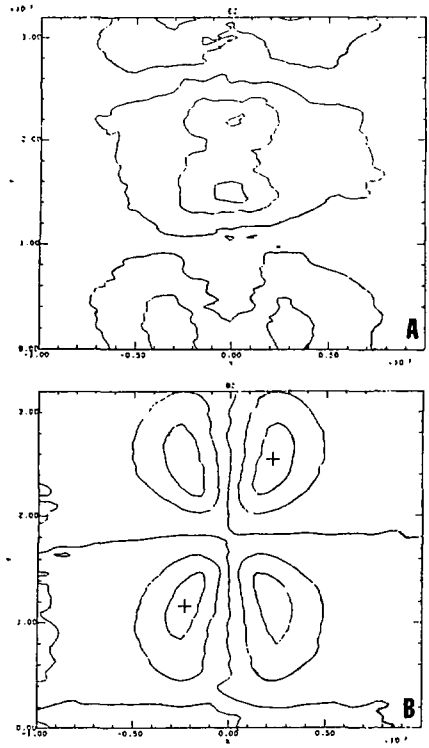

Figure 2. The normal component of the (a) electric field consistent with the magnetic flux configuration of Fig. 1d and (b) the magnetic quadrupole struture of the normal component of the magnetic field for the same configuration.

ions attempting to follow the electrons into the O-point, pulled by an ambipolar electric field. For large ion-to-electron mass ratios (> 200), the electron flow reverses before the ions can neutralize the excess electronic charge. These curves are shown in Figure 3 for six different values of M_i/m_e.

Late in time after the oscillations damp out, the trapped flux grows approximately linearly in time, at a rate proportional to the ion-acoustic speed, $v_s = (kT_e/M_i)^{1/2}$. (Consistent with this scaling, in the limit $M_i/m_e \rightarrow \infty$ the trapped flux experiences simple oscillation with no secular growth.) This late-time oscillation and secular growth of trapped flux is a qualitatively different phenomenon than has been

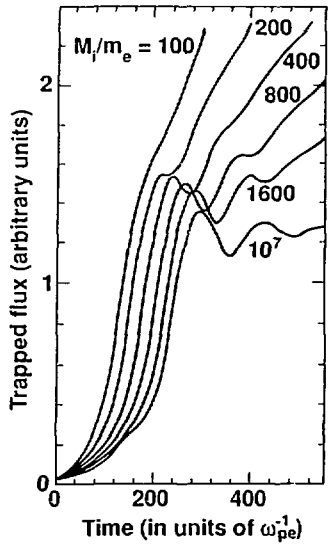

Figure 3. Trapped magnetic flux vs time, for six different M_i/m_e. In all cases, $T_{e\parallel}/T_{e\perp} = 4/9$ initially. The long-time linear growth is proportional to $M_i^{-1/2}$.

reported in previous studies.[5] Previous investigators, using M_i/m_e=10–25, saw the coalescence of small-scale magnetic islands and sometimes saw oscillatory behavior, but after the island began to interact with the outer wall. Inadequate separation between the ion and electron timescales would obscure the late time oscillations that we see resulting from charge separation electric fields and from $\mathbf{E} \times \mathbf{B}$ forces, superposed on continued secular growth of trapped flux (Figure 3).

The nature of the three temporal regions described above for $M_i/m_e > 200$ can be clarified by an idealized simulation having $T_{e\parallel}/T_{e\perp} = 0$, and $M_i/m_e = 2000$. Figure 4 shows the time evolution of a) trapped magnetic flux, b) quadrupole z component of magnetic field, c) electron flow energy in the y- and z-directions, and d) z components of electric field and current. Region I, in which the trapped flux grows linearly with time, corresponds to the early electron-driven formation of small-scale current filaments as evidenced in Figure 1(b). Region II corresponds to the coalescence of the small-scale multiple X-points, and shows exponential growth of trapped flux. The end of region II is signaled by a peak in y-directed electron energy consistent with jetting, and a corresponding reduction of the z-directed energy caused by the E_z required for the jetting. In Region III, ions play the decisive role: an ambipolar electric field between the electrons and much-more-massive ions reverses the electron flow, causing oscillations back and forth from the external region through the X-

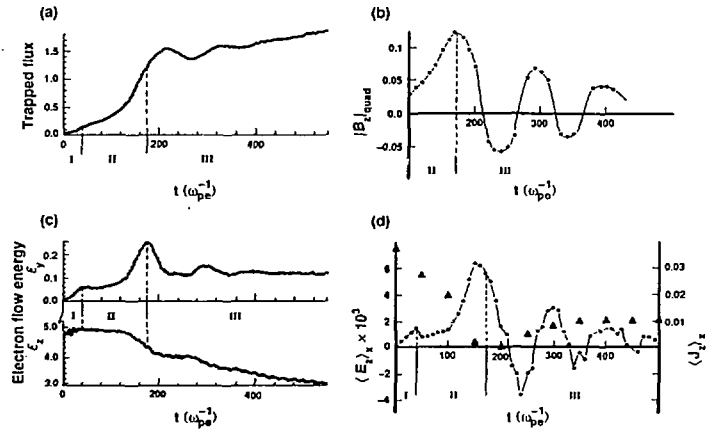

Figure 4. Time evolution of an idealized simulation with initial $T_{e\parallel}/T_{e\perp} = 0$ and $M_i/m_e = 2000$: (a) trapped magnetic flux; (b) peak-to-peak amplitude of quadrupole magnetic field B_z; (c) electron flow energy in the y- and z-directions versus time; and (d) E_z (dots) and J_z (triangles) at the y-position of the X-point, averaged over x.

point to the O-point. These oscillations are seen most clearly in Figure 4(b).

The oscillations that are evident in the z component of the electric field, Figure 4(d), are not found in the z component of the current. In fact there is no proportionality at all between the time behaviors of E_z and J_z. The z components of the current and electric field do not even occupy the same volume in our simulations. Early in the reconnection process the electrons that carry J_z move away from the X-points, and subsequent currents flow in the vicinity of the O-points. This behavior is seen in laboratory reconnection experiments as well.[11] Even if there were an "anomalous resistivity" η, the rate of dissipation ηJ^2 would be quite small at the X-point, since J_z is small there. Thus the MHD picture with an "anomalous resistivity" η acting on the z-component of current at the X-point seems to be qualitatively incorrect for the cases we have examined here. There remains, however, the more speculative possibility that "anomalous" dissipation might operate on the oscillating electron currents in the x-y plane.

3. DISCUSSION

The results of the present work agree qualitatively with behavior seen in previous computer simulations[5] at early and intermediate times : 1) initial formation of small-scale magnetic islands, and 2) rapid coalescence of these into larger structures, with concomitant development of a driving E_z. We observe a new type of behavior at later times, for ion-to-electron mass ratios above 200: oscillatory electron currents through the X-point in the x-y plane, superimposed on linear (not exponential) growth of trapped flux at a rate proportional to $(T_e/M_i)^{1/2}$.

The distinction between regions I and II in Fig. 4 is the linear, rather than exponential, growth of trapped flux at early time. Previous speculation[1] that the distinction is *not* due to the extreme initial anisotropy ($T_{e\parallel}/T_{e\perp} = 0$) has been proven. Shown in Fig. 5a are plots of trapped flux for two runs starting with anisotropies having the extreme value of 0 and our canonical value of 4/9. The qualitative

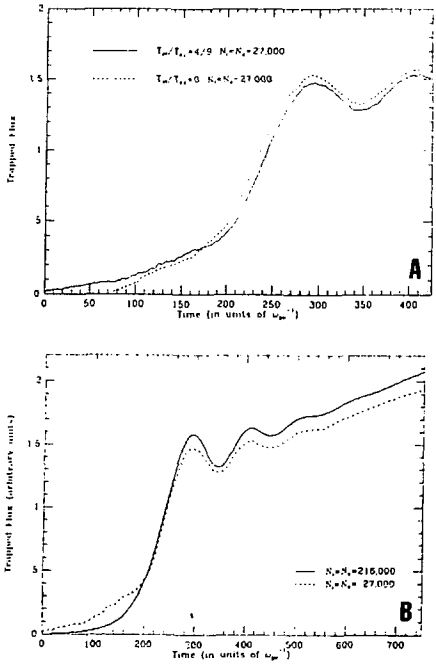

Figure 5. Trapped magnetic flux vs time with (a) all parameters equal except for different $T_{e\parallel}/T_{e\perp}$. Shown in (b) is a comparison with $T_{e\parallel}/T_{e\perp} = 4/9$ but with one run having an order of magnitude more particles.

similarity of the two runs throughout the time and especially in the early time surrounding regions I and II affirm our early speculation.

The second more likely possibility for the distinction between regions I and II is that the large fluctuation noise is associated with the limited number of simulation particles ($N_e = N_i = 27,000$). This noise provides very early "reconnection" with sufficient amplitude to obscure the early exponential growth. Simulation of this problem with ($T_{e\parallel}/T_{e\perp} = 4/9$) and an order of magnitude more particles ($N_e = N_i = 216,000$) does indeed show exponential growth (Fig. 5b) and the absence of the linear growth of region I. Further, we find the exponential growth to be consistent with the linear collisionless electron-driven tearing mode instability[12].

The evidence is that simple fluctations near the field

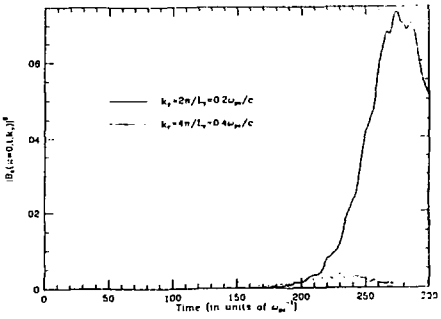

Figure 6. Time histories of the Fourier amplitudes for the many particle run shown in Fig. 5b. The most unstable mode $k_y = 0.2\omega_{pe}/c$ clearly dominates the mode with half the wavelength $k_y = 0.4\omega_{pe}/c$ that appears to be the most unstable early in the high noise runs (as in Fig. 1b).

null cause small scale islands to form with amplitudes proportional to the initial particle noise level. These early islands, through not the most unstable length in y, dominate the simulation until the exponential growth of the most unstable island length overtakes the growth of the early perturbations. Large numbers of simulation particles suppress the initial noise-related perturbations and exhibit only exponential growth of the most unstable mode. This result is further supported by examining the Fourier spectrum in y of B_z in Fig. 6 that shows the linearly-predicted most unstable mode dominating the mode with one-half the wavelength.

We note that the simulation with fewer particles displays excellent qualitative agreement (see Fig. 5b) for those phenomena occuring in the nonlinear regime–providing confidence for further study with relatively inexpense simulations using fewer simulation particles.

Our simulations indicate that the region showing oscillatory behavior (Region III of Fig. 4a) is one in which an electron current flows into and out of the O-points through the X-points. The ions attempt to follow the electron current, pulled by an ambipolar electric field. But only for small ion-to-electron mass ratios (< 200) can they succeed in doing so before the electron flow reverses. Such behavior emphasizes that in our simulations the magnetic flux is frozen into the *electron* component rather than the plasma as in the usual MHD formulation.

This research was performed under the auspices of the U.S. Department of Energy by the Lawrence Livermore National Laboratory under contract no. W-7405-ENG-48.

References

[1] D.W. Hewett, G.E. Francis, and C.E. Max, "New Regimes of Magnetic Reconnection in Collisionless Plasmas", Phys. Rev. Lett. **61**, 893, August 15, (1988).

[2] F.V. Coroniti and C.F. Kennel, J. Geophys. Res. **77**, 3361 (1972), and in *Cosmic Plasma Physics*, edited by K. Schindler (Plenum, NY, 1972), page 15; C.T. Russell and R.L. McPherron, Space Sci. Rev. **15**, 205 (1973); K. Schindler, in *Dynamics of the Magnetosphere*, edited by S.-I. Akasofu (Reidel, Hingham, Mass., 1980), page 311.

[3] L.L. Cowie and C.F. McKee, Astrophys. J. **211**, 135 (1977).

[4] R.L. Stenzel and W. Gekelman, J. Geophys. Res. **86**, 649 (1981); W. Gekelman and R.L. Stenzel, J. Geophys. Res. **86**, 659 (1981).

[5] J.N. Leboeuf, T. Tajima, and J.M. Dawson, Phys. Fluids **25**, 784 (1982); J.N. Leboeuf et al., in *Magnetic Reconnection in Space and Laboratory Plasmas*, edited by E.W. Hones (Am. Geophys. Union, Washington DC, 1984), pg. 282; M. Hoshino, J. Geophys. Res. **92**, 7368 (1987).

[6] D.W. Hewett and A.B. Langdon, J. Comp. Phys. **72**, 121 (1987).

[7] R.L. Stenzel and W. Gekelman, Phys. Rev. Lett. **42**, 1055 (1979).

[8] E.G. Harris, Nuovo Cimento **23**, 115 (1962).

[9] J. Chen and P. Palmadesso, Phys. Fluids **27**, 1198 (1984).

[10] M. Hoshino, op. cit.

[11] W. Gekelman and H. Pfister, Bull. Am. Phys. Soc. **32**, 1753 (1987).

[12] G. Laval, R. Pellat, and M. Vuillemin, in *Plasma Physics and Controlled Nuclear Fusion Research* volume 2 (I.A.E.A., Vienna, 1966), page 259; See also summary in Hones (ref. 5), pages 311-315.